



Published in final edited form as:

Pediatr Res. 2022 December ; 92(6): 1580–1589. doi:10.1038/s41390-022-02002-1.

Metabolome and Microbiome Multi-omics Integration from a Murine Lung Inflammation Model of Bronchopulmonary Dysplasia

Ahmed El Saie^{*,1}, Chenlian Fu^{*,2,5}, Sandra L. Grimm^{3,5,6}, Matthew J Robertson³, Kristi Hoffman⁴, Vasanta Putluri⁵, Chandra Shekar R Ambati⁵, Nagireddy Putluri⁵, Binoy Shivanna¹, Cristian Coarfa^{#,3,5,6}, Mohan Pammi^{#,1}

¹Section of Neonatology, Department of Pediatrics, Baylor College of Medicine and Texas Children's Hospital, Houston, Texas

²Department of Biology, Harvey Mudd College, Claremont, California

³Dan L Duncan Comprehensive Cancer Center, Baylor College of Medicine, Houston, Texas

⁴Alkek Center for Metagenomics and Microbiome Research, Baylor College of Medicine, Houston, Texas

⁵Department of Molecular and Cellular Biology, Baylor College of Medicine, Houston, Texas

⁶Center for Precision Environmental Health, Baylor College of Medicine, Houston, Texas

Abstract

Background: Respiratory tract microbial dysbiosis can exacerbate inflammation and conversely inflammation may cause dysbiosis. Dysbiotic microbiome metabolites may lead to bronchopulmonary dysplasia (BPD).

Hypothesis: Hyperoxia and lipopolysaccharide (LPS) interaction alters lung microbiome and metabolome, mediating BPD lung injury sequence.

Methods: C57BL/6J mice were exposed to 21% (normoxia) or 70% (hyperoxia) oxygen during postnatal days (PND) 1–14. Pups were injected with LPS (6 mg/kg) or equal PBS volume, intraperitoneally on PND 3, 5, and 7. At PND14, lungs were collected for microbiome and metabolomic analyses (n=5/group).

Corresponding author: Cristian Coarfa, PhD, Dept. of Molecular and Cellular Biology, Dan L Duncan Comprehensive Cancer Center, Center for Precision Environmental Health, Baylor College of Medicine, Houston, Texas, 77030, Telephone 713-798-7938, coarfa@bcm.edu.

*co-first authors and contributed equally to the manuscript

#co-senior authors

Author Contributions

All authors included in this paper fulfil the criteria of authorship. M.P. conceived the ideas. A.E.S., B.S., and M.P. collected the samples. K.H., V.P., C.S.R.A., N.P. processed the samples and performed the omics profiling. A.E.S., C.F., S.L.G., M.J.R., C.C., and M.P. analyzed the data. A.E.S., C.F., C.C., S.L.G., and M.P. prepared the first draft. All authors have read and approved the current version.

Disclosure statement: We have no conflicts of interest to disclose.

Consent Statement: Patient consent was not required.

Results: Microbiome alpha and beta diversity were similar between groups. Metabolic changes included: hyperoxia 31 up/18 down, LPS 7 up/4 down, exposure interaction 8. Hyperoxia increased *Intestinimonas* abundance, whereas LPS decreased *Clostridiales*, *Dorea*, and *Intestinimonas*; exposure interaction affected *Blautia*. Differential co-expression analysis on multi-omics data identified exposure-altered modules. Hyperoxia metabolomics response was integrated with a published matching transcriptome, identifying four induced genes (*ALDOA*, *GAA*, *NEU1*, *RENBP*), which positively correlated with BPD severity in a published human newborn cohort.

Conclusions: We report hyperoxia and LPS lung microbiome and metabolome signatures in a clinically relevant BPD model. We identified four genes correlating with BPD status in preterm infants that are promising targets for therapy and prevention.

Introduction

The human microbiome project has enhanced our understanding of the human microbiome and its relation to health and disease¹. The development and the normal progression of the respiratory microbiome is crucial for health, and conversely its perturbation is associated with respiratory disease^{2–5}. Recent evidence indicates that the microbiota colonize the respiratory tract at birth and may even be present in the fetal lungs^{6,7}. The diversity and composition of the lung microbiome evolve in the first months of life and disruption and imbalance of microbial communities (dysbiosis) may exacerbate inflammation leading to respiratory diseases in infants and children^{4,7}. This may be mediated by microbial metabolites such as short chain fatty acids or tryptophan catabolites⁸. Conversely, inflammation has been shown to impact the development and normal progression of microbial communities in the lung⁹. Very few studies have reported microbiome-metabolome integration after lung inflammation that might help us understand the pathophysiology of bronchopulmonary dysplasia (BPD), which is characterized by interrupted lung development and alveolar simplification^{10,11}.

Excessive supplemental oxygen (O₂) use or hyperoxia leads to BPD by disrupting growth factor signaling, extracellular matrix assembly, cell proliferation, and vasculogenesis¹³. Multiple studies have shown that hyperoxia-induced lung parenchymal and vascular injury in neonatal mice leads to a phenotype similar to that of human BPD with pulmonary hypertension¹⁴. Another insult that leads to inflammation is infection or colonization with pathogens. Lipopolysaccharide (LPS, also termed endotoxin), a component of the outer membrane of gram-negative bacteria leads to systemic and lung inflammation. LPS activates airway epithelial cells, neutrophils, and alveolar macrophages, resulting in the release of inflammatory mediators, such as reactive oxygen species (ROS), tumor necrosis factor- α (TNF- α), and interleukin-6 (IL-6)¹⁵. In an LPS-induced ARDS model in male rats, comparison between the LPS-treated rats and the control group revealed changes in metabolites associated with oxidative stress³². In another experiment, a rat model of ventilator induced lung injury, the metabolomic assay was able to capture multiple metabolites associated with this injury in serum³³. Since hyperoxia and multiple doses of LPS were both demonstrated to produce BPD phenotypes, we used a double-hit mice model to study the impact of the two factors (hyperoxia and LPS) on mice lung microbiome and metabolome^{17,34} (Figure 1).

Investigating and integrating changes in microbiome and metabolome related to BPD risk factors and the interplay between such changes provides a unique opportunity to gain insights into the pathogenesis of BPD and respiratory diseases in general²⁸. Based on fore-mentioned double-hit mice model, we report multiple lung microbiome genera and lung metabolites that were influenced by hyperoxia, LPS or the interaction between the two factors. Differential Correlation Expression Analysis (DiffCoEx)³⁵ were performed to find subsets of microbiomes and/or metabolites whose response to one of the two factors might be similar, and thus might interact with each other. Using a published transcriptomic profile of a matching hyperoxia exposure model³⁶, we determined genes associated with our hyperoxia metabolic response using the MetaboAnalyst server³⁷. We then evaluated the association of gene signatures with clinical variables of interest, including BPD status, need for oxygen, birth weight, and gestational age from a published blood transcriptomic cohort from human newborns at risk of BPD³⁸. We specifically identified 4 genes that may play a major role in disease pathogenesis after hyperoxia induced inflammation. The effect of hyperoxia and LPS on the microbiome and metabolome of mice in the double-hit model used is clinically relevant to the development of BPD in preterm infants.

Methods

Animal model of hyperoxia and LPS induced lung inflammation:

We used a double hit model of lung inflammation during the saccular and alveolar phases of lung development that was an adaptation from animal models previously reported^{17,34} (Figure 1). This study was approved by the Institutional Animal Care and Use Committee of Baylor College of Medicine and conducted as per American Physiological Society (2010–2011) guidelines for animal studies. C57BL/6/J WT mice were obtained from the Jackson Laboratory (Bar Harbor, ME). Mice raised from timed pregnancy in our facility were used. Male and female pups were collected from various litters and then reallocated to the dams before being exposed to 21% oxygen (normoxia) or 70% oxygen (hyperoxia) during postnatal days (PNDs) 1–14. Plexiglass chambers were used to perform the hyperoxia experiments, into which oxygen was delivered continuously through an oxygen blender to reach a steady continuous level of 70% oxygen. Every 24 hours, the dams were switched between the normoxia and hyperoxia exposed litters during the exposure period to prevent oxygen toxicity in the dams and to control maternal effects between the groups. The pups were injected with 6 mg/kg of *Escherichia coli* O55:B5 LPS (Sigma-Aldrich, St. Louis, MO; Cat No. L2280) or an equivalent volume of control vehicle (PBS), intraperitoneally on postnatal days (PNDs) 3, 5, and 7 while they were being exposed to normoxia or hyperoxia through PNDs 1–14. Thus, 20 pups were distributed into 4 experimental groups each containing 5 pups (normoxia and LPS, normoxia and PBS, hyperoxia and LPS, hyperoxia and PBS). At PND 14, the animals were euthanized using intraperitoneal injections of 200 mg/kg of sodium pentobarbital, and the lung tissues were collected for microbiome and metabolome analyses (Figure 1).

Microbiome analysis:

Lung microbiome was evaluated by 16S rDNA sequencing at the Alkek Center for Metagenomics and Microbiome Research (CMMR) (<https://www.bcm.edu/research/centers/>)

metagenomics-and-microbiome-research). Genomic DNA was extracted from lung tissue using the PowerLyzer Tissue & Cells Kit (Qiagen), amplified by PCR, and sequenced on an Illumina MiSeq using the 2×250 bp paired-end protocol. Primers used for amplification (515F/806R) targeted the V4 region and contained adapters for MiSeq sequencing along with a single-index molecular barcode on the reverse primer. Resulting read pairs were demultiplexed based on their molecular barcode and merged using USEARCH v7.0.100³⁹, allowing zero mismatches with a minimum overlap of 50 bases. Merged reads were trimmed at first base with Q5 and reads containing above 0.05 expected errors were removed. Sequences were assigned into Operational Taxonomic Units (OTUs) at an identity cutoff value of 97% using the UPARSE algorithm⁴⁰. To determine taxonomies, OTUs were mapped to an optimized version of the SILVA Database⁴¹(v.128) containing only the 16S v4 region. A custom script constructed an OTU table from the output files generated in the previous steps. The data have been deposited with links to BioProject accession number PRJNA800055 in the NCBI BioProject database (<https://www.ncbi.nlm.nih.gov/bioproject/>).

Analysis and visualization of microbiome communities was conducted in the statistical platform R, utilizing the phyloseq package⁴² to import sample data and calculate alpha and beta diversity metrics. Microbiome genera with relative abundance above of 0.5% were analyzed using the two-way ANOVA test, without post-hoc analyses, with significance achieved at p-value < 0.05, using the R statistical system. Boxplots of significant microbiota associated with independent factors or with factor interaction were generated using GraphPad Prism version 9.1. Alpha- and beta- diversity association with either hyperoxia or LPS exposures was assessed using PERMANOVA via the vegan R package⁴³.

Metabolome Analysis:

Metabolome analysis was performed using mass-spectrometry at the Metabolomics Core, Baylor College of Medicine. Metabolites were extracted from cell pellets using previously described standard procedures for targeted metabolomic profiling using ultra high-performance liquid chromatography/tandem-mass spectrometry^{44–47}. The extracted samples were analyzed using high performance liquid chromatography (HPLC) coupled to Agilent 6495 QQQ mass spectrometry. The data was normalized with respect to the internal standards on a per-sample basis then log2-transformed. Metabolome data was then analyzed using the two-way ANOVA test, with significance achieved at FDR-corrected p-value < 0.05, using the R statistical system. Heatmaps of significant microbiota associated with independent factors or with factor interaction were generated using the R statistical system. Enriched pathway analysis was performed on metabolites identified to show significant differences due to each differing clinical condition using the MetaboAnalyst server³⁷.

Correlation-based Bioinformatics Analysis:

We utilized the statistical workflow DiffCoEx³⁵ to identify and visualize groups or modules of metabolites, microbiota, or combined modules of metabolites and microbiota combined that show a significant change in correlation between different experimental conditions. The experimental groups were defined based on either oxygen exposure (normoxia versus hyperoxia) or toxin exposure (LPS versus PBS). We explored yet unappreciated systems

biology associations of the metabolites, microbiota, or mixed metabolites and microbiota present in the same module and in the same experimental condition.

We assessed the correlation between the above-mentioned significant microbiota genera and the significant metabolites. For each exposure (hyperoxia or LPS), a microbiome vs. metabolome Spearman rank correlation matrix⁴⁸ was constructed and visualized with the heatmap library⁴⁹ as implemented in the R statistical system and with GraphPad Prism version 9.1.

Clinical association with BPD status:

Using a transcriptomic gene signature of hyperoxia from a matched murine model of hyperoxic lung injury³⁶, we determined genes associated with our hyperoxia metabolic response using the MetaboAnalyst server³⁷. Next, we used a blood transcriptomic cohort from human newborns at risk of BPD³⁸ to evaluate the association of gene signatures with clinical variables of interest, including BPD status, need for oxygen, birth weight, and gestational age. A gene signature score was computed for each specimen in the cohort as follows: each gene was converted to a z-score, then z-scores of up-regulated genes were added followed by subtraction of z-scores for down-regulated genes. Association between gene signature scores and clinical variables was performed using Pearson's Correlation Coefficient, with significance achieved at $p < 0.05$. Multivariable analysis of association with BPD status and with oxygen therapy was conducted using the lm package in the R statistical system.

Results

Exposure to hyperoxia or LPS-induced inflammation altered the microbial relative abundances in the murine lung

Hyperoxia exposure and LPS injection both impacted the murine lung microbiome. Specific microbiota whose relative abundance were significantly altered after hyperoxia exposure or LPS injection were identified through a parametric two-way ANOVA test (Table 1). Hyperoxia exposure was associated with a significantly increased the abundance of *Intestinimonas*, whereas LPS exposure was associated with a decreased the relative abundance of 3 genera: *Clostridiales* (Unc04zd2), *Dorea*, and *Intestinimonas*; the relative abundance of *Blautia* was significantly associated with the interaction of these two exposures (Figure 2 A–C). Mice lung microbiome composition across all four groups show that the phylum *Firmicutes* comprised 98.4%, the class *Clostridia* comprised 96.5%, and the order *Clostridiales* comprised 96.2% respectively of all mice lung microbiome profiled. Potentially due to the dominance of *Firmicutes*, there were no statistically significant differences observed for either alpha diversity or beta diversity associated with hyperoxia exposure or LPS injections (Figure 4 A–C).

Exposure to hyperoxia or LPS-induced inflammation was associated with significant changes in the metabolites of the murine lung

Hyperoxia exposure and LPS injection both impacted metabolite expression in murine lungs. Specific metabolites altered significantly by hyperoxia exposure or LPS treatment

were identified through a parametric two-way ANOVA test (Table 1) and visualized using hierarchical clustering (Figure 2 D–E). Hyperoxia exposure was associated with upregulation of 31 metabolites and down regulation of 18 metabolites, with top enriched metabolic pathways including glycine, serine, and threonine metabolism, arginine biosynthesis, and glycerophospholipid metabolism (Supplementary Figure S1). LPS exposure was associated with upregulation of 7 metabolites and downregulation of 4 metabolites, also enriching for glycine, serine, and threonine metabolism, and for arginine biosynthesis (Supplementary Figure S1). Finally, 8 metabolites were significantly associated with the interaction of these two exposures, with purine metabolism the top enriched pathway (Supplementary Figure S1).

A multi-omic interaction map for exposure-associated microbiome and metabolome

Whereas we identified the significant microbiome genera and significant metabolites associated with hyperoxia or LPS exposures, systemic associations between microbiome genera and metabolites are yet unappreciated. Using Spearman rank correlations, we generated the interaction map between microbiome genera and metabolites associated with each individual exposure. Specifically, we computed correlations between hyperoxia associated microbiome and metabolites in the normoxia and hyperoxia group (Figure 3A). Similarly, we computed correlation between the LPS associated microbiome and metabolites in the PBS and LPS treatment groups (Figure 3B). This analysis provides more nuanced insights on exposure-specific individual metabolite-microbiome interactions. Our analysis reveals that normoxia samples show different microbiome-metabolome correlation than hyperoxia samples. Interestingly, *Intestinimonas* shows similar patterns of correlation with metabolites in the PBS and LPS sample groups, but *Clostridiales* (Unc04zd2) and *Dorea* show distinct correlation patterns.

Differential co-expression analysis identifies novel exposure-associated single-omic and multi-omic modules

By conducting multi-omics profiling on lung microbiome and lung metabolome from the same mice, we were able to probe systematic yet unappreciated relationships between microbiome and metabolites. Specifically, we conducted differential co-expression analysis using DiffCoEx³⁵ on both single-omic (Figure 5A–D) and multi-omic profiles (Figure 5E–F). Modules were considered significant at $p < 0.05$ after performing permutation testing using 1000 permutations (Supplementary Figure S2, Supplementary Table 1). A module that gained or lost correlation after a particular exposure could represent either a direct exposure effect or a systemic adaptation of the murine host. In particular, metabolites or microbiota in a gained or lost module might impact one another in a functional network. For microbiome only analysis, we noticed a pink module of 73 genera gains correlation after LPS exposure, whereas a brown module of 17 metabolites loses correlation. Similarly, at metabolite level, the turquoise module of 28 metabolites loses coherence after LPS exposure, whereas both the brown module (18 metabolites) and blue module (19 metabolites) gain coherence. We then conducted DiffCoEx⁵³ on combined microbiome and metabolome data. In the multi-omic DiffCoEx analysis, LPS exposure led to more robust module changes (Supplementary Figure S2 E–F), in particular lost correlation in a brown module of 28 features, all of which are microbiome features, with 10 of them belonging to the Family Lachnospiraceae.

An integrated transcriptomics and metabolomics signature of hyperoxia associates with BPD risk.

We have shown previously⁵⁰ that hyperoxia signatures derived in neonatal murine models associate with BPD risk in blood transcriptome from human newborns³⁸. Using the metabolomic profiling conducted in the current study, we integrated it with a transcriptomic signature from an age matched murine study³⁶. Specifically, we utilized MetaboAnalyst to identify genes associated with metabolites significantly altered by hyperoxia exposure. The human study assessed 111 newborns, with a mean birth weight of 1029g (SD, 290), and a mean gestational age of 27.8 weeks (SD, 2.5)³⁸. Blood samples drawn on 5th, 14th and 28th day of life were evaluated for gene expression. Infants with bronchopulmonary dysplasia (n=68), defined as per Jobe & Bancalari⁵¹, were compared with controls (n=43). We assessed association with several clinical variables of interest, including BPD status, birth weight, gestational age and oxygen therapy (defined as whether oxygen was administered or not for a period greater than or equal to 28 days). Our analysis determined that the complete transcriptomics signature previously reported, positively associated with BPD status (Pearson correlation coefficient, p-value<0.05) (Figure 6A). Next, we identified four genes both induced in the previously reported hyperoxia transcriptome and associated with hyperoxia altered lung metabolites, specifically *Aldoa*, *Gaa*, *Neu1*, and *Renbp*, that were positively correlated both as a single gene and as a combined gene signature with BPD status and oxygen requirement but negatively correlated with birth weight and gestational age (Figure 6A). Detailed analysis for association with BPD status was presented via scatterplots for the complete transcriptomics signature, for each of the individual four genes, and for the combined four-gene signature (Figure 6B). We performed multi-variable analysis for the association with BPD status and with oxygen therapy incorporating the demographic variables birth weight and gestational age; we showed that *Neu1* achieved a p=0.092 and the 4 gene signatures achieved a p=0.118 for BPD status association using multivariable analysis (Supplementary Table 2).

Discussion

We report the microbiome and metabolome signatures in response to lung inflammation in a double-hit murine model (hyperoxia and LPS exposure) of lung inflammation and BPD. We identified modules of metabolites and microbial genera that are altered in lock-step in response to individual exposure by using differential co-expression analysis (DiffCoEx). We also report an integrated analysis of our metabolic profiling in conjunction with published transcriptome data from lungs of age-matched mice with a similar hyperoxia exposure. Our analysis revealed 4 genes that associate with the development of BPD using blood transcriptome from a human newborn cohort.

The reported changes in metabolic and microbiome signatures are significant as most of the published microbiome and metabolomic studies have focused on adult lung diseases including ARDS and COPD with few data on the neonatal lung inflammation and injury⁵. We report here the changes in metabolic signatures in the lung in a murine double-hit model of experimental BPD, and evaluate the affected biological pathways regulated via metabolomics changes. The lung of neonatal mice are similar to the structure of the

developing human lungs and are at the saccular stage of development⁵⁰. Together with the inflammation that results from hyperoxia exposure with LPS injection, the oxidative stress results in a phenotype similar to the bronchopulmonary dysplasia and hence we decided to use this double hit model⁵².

We report microbial genera that are associated with hyperoxia and LPS exposure in our murine model of lung inflammation. We first highlight the dominance of Order Clostridiales (Phylum Firmicutes) whose relative abundance is consistently high for all mice studied and averages at ~96.2% of all microbial counts. We identified more microbial genera whose relative abundances change significantly due to LPS vs. PBS when compared with hyperoxia vs. normoxia (three LPS-associated genera versus one hyperoxia-associated genera). Furthermore, differential co-expression analysis using DiffCoEx identified modules of microbiome genera that are changed robustly after LPS exposure compared to only minor changes in co-expression after hyperoxia exposure. Unlike studies that reported differences in the microbial diversity and abundance (alpha and beta diversity) between patients with BPD and controls^{6,54}, we did not find a difference in the alpha and beta diversity after LPS or/and hyperoxia exposures in this murine model of BPD, possibly due to the dominance of Order Clostridiales (Phylum Firmicutes). An airway microbiome is present at birth in preterm neonates which may prime the immune system and its perturbation may result in BPD^{6,7}. Early airway metagenomic and metabolomic signatures that associate with BPD have been described⁵⁵. Reports on airway microbiome immediately after birth show that there is an evolution of microbial colonization, with increases in bacterial DNA loads during the first weeks of life, with older infants with established BPD had more diverse microbiomes compared with preterm infants at birth⁷. Ashley et al, in an elegant study describe the effects of hyperoxia on lung injury and dysbiosis⁹. After hyperoxia, dysbiosis precedes lung injury suggesting dysbiosis might have an impactful role in lung injury, further supported by experiments reporting that germ-free mice are protected to hyperoxic lung injury⁹. These findings provide insight on the pathogenesis of BPD in preterm infants who are exposed to high concentrations of oxygen, often on antibiotics that cause dysbiosis. Interestingly, in contrast to the microbiome analysis, hyperoxia exposure produces a more profound impact on the murine lung metabolome. We identified more metabolites whose levels change significantly due to the hyperoxia compared to LPS (49 metabolites identified for hyperoxia compared to 11 metabolites identified for LPS exposure). Similarly, differential co-expression analysis using DiffCoEx⁵³ revealed more metabolites included in modules that are changed in lock-step after hyperoxia exposure compared to the number of metabolites included in modules that respond to the LPS; interestingly, the changes in correlation were stronger after LPS exposure, at both microbiome and metabolome level. While the effect of both exposures on individual metabolic and microbiome networks is robust, neither exposure shows a statistically significant impact on community-level microbiome diversity.

Hyperoxia produced a significant change in the metabolomic map in this BPD mouse model, and the interaction between LPS and hyperoxia led to a profound effect on the metabolites. Gentle et al have reported decreased nitrate reductase activity in the oral cavity of preterm infants with BPD⁵⁷. Previously, Pintus et al. and Fanos et al., identified multiple metabolites including trimethylamine-N-oxide (TMAO), alanine, betaine, lactate, taurine and glycine

as distinct metabolites between controls and BPD patients^{58,59}. Taurine is important in apoptosis, detoxification and calcium homeostasis, with glycine being crucial in synthesis of glutathione and its antioxidant role⁶⁰. Our study matches with these studies by identifying several alanine variants, namely Phenyl alanine, N-acetyl alanine, Methyl alanine, as well as betaine, glycine, and N, N Dimethyl Glycine to be metabolites whose levels changed significantly under the impact of hyperoxia. Conversely, N, N Dimethyl Glycine levels changed significantly under the impact of LPS, whereas lactate levels associated with the interaction between hyperoxia and LPS. We also note that multiple metabolites in the carnitine family have levels impacted significantly by hyperoxia and/or LPS, such as Octonyl Carnitine and 2-Methylbutyrylcarnitine, whereas Acetyl Carnitine, Butyryl Carnitine, and carnitine levels were significantly altered only by hyperoxia exposure. This agrees with an existing mice-model paper which concludes that the deletion of the gene coding for carnitine palmitoyl transferase that limits the shuttling rate of carnitine can augment oxygen-induced apoptosis⁶¹. Identifying these changes in metabolites and amino acids in BPD neonates, may outline key metabolic pathways that may be amenable for prevention or ameliorating the disease pathogenesis.

The reconfiguration of micro-metabolic landscape due to inflammation may regulate gene expression⁶¹. The effects of such landscape have been demonstrated in multiple processes in the human body including oncogenesis and embryological development, and it may play a role in lung injury and repair. Metabolomic signatures have led to discovery of novel therapies in cancer biology^{54,62}; however, these signatures are not well characterized in BPD. In this study, by integrating our metabolomic response to hyperoxia with a publicly available gene signatures from age-matched and exposure-matched mouse lung, we identified four genes involved in metabolism ALDOA (aldolase A), GAA (alpha glucosidase), NEU1 (neuraminidase 1), and RENBP (renin binding protein), that both individually and as a group associate with BPD severity in a blood transcriptomic cohort from human newborns at PND28. ALDOA, GAA, and NEU1 have been linked with pulmonary conditions or diseases according to existing literature. ALDOA is a key glycolytic enzyme and is a strong driver gene for lung, pancreatic and hepatocellular cancers, GAA (mutations of alpha glucosidase cause Pompe's disease a lysosomal storage disease causes smooth muscle dysfunction in trachea and bronchi and has been known to be related to asthma^{61,65,66}. NEU1 has been expressed in lung microvasculature, shown to restrict endothelial cell migration and associated with idiopathic pulmonary fibrosis^{67,68}... RENBP has been shown to be expressed in lungs and its expression changes significantly under sodium depletion and captopril administration in mice^{61,69} underlining the role for fluid status and BPD exacerbation. It is not clear how the four identified genes affects the microbiome-metabolome interactions or inflammation and need further studies.

A limitation of our study is that there are inherent differences in the microbiome between humans and animals but among rodent models, human microbiome is closest to mice⁵³. Extrapolation of results from the mice to the human will have to be done with caution. Another limitation is the small sample size in the groups, and we may be underpowered to detect important differences among the groups. Comparing datasets and proteomic signatures between blood and lung has to done with caution. In a study evaluating transcriptomic profiles from blood and lung after exposure to carbon nanoparticles, lung

profile was not completely replicable in whole blood, but specific systemic responses were shared⁷⁰.

Dysregulation of microbiome and metabolomic landscape may contribute to the response to hyperoxia- or LPS- induced health sequela. In addition to illustrating the microbiome landscape of mice lung and how it is impacted by hyperoxia and LPS, we identified robust metabolic-related responses to individual treatments with hyperoxia or LPS, as well as combined hyperoxia/LPS treatment, much remain to be learned on if and how the metabolome and microbiome can therapeutically be targeted to improve the outcomes of respiratory disorders including BPD. By integrated analysis with published literature, we identified 4 candidate genes that can be further studied in the context of microbial dysbiosis and inflammation and potentially act as targets for BPD prevention or treatment.

Supplementary Material

Refer to Web version on PubMed Central for supplementary material.

Acknowledgements

MP is funded by NIH grants, R03HD098482 and R21HD091718. The metabolomics core was supported by the CPRIT Core Facility Support Award RP170005 "Proteomic and Metabolomic Core Facility," NCI Cancer Center Support Grant P30CA125123, NIH/NCI R01CA220297, NIH/NCI R01CA216426 intramural funds from the Dan L. Duncan Cancer Center (DLDC). FC and CC were partially supported by was partially supported by The Cancer Prevention Institute of Texas (CPRIT) RP170005, NIH P30 shared resource grant CA125123, and NIEHS center grants P30 ES030285 and P42 ES027725, and NIMHD P50MD015496.

Statement of financial support.

This study was funded by the following extramural sources:

NIH R03HD098482, R21HD091718, CA125123; NCI P30CA125123; NIH/NCI R01CA220297, R01CA216426; NIEHS P30 ES030285, P42 ES027725, NIMHD P50MD015496; CPRIT RP170005

References

1. The Integrative Human Microbiome Project: Dynamic Analysis of Microbiome-Host Omics Profiles During Periods of Human Health and Disease. *Cell Host Microbe* 16, 276–289 (2014). [PubMed: 25211071]
2. Dickson RP et al. The Lung Microbiota of Healthy Mice Are Highly Variable, Cluster by Environment, and Reflect Variation in Baseline Lung Innate Immunity. *American journal of respiratory and critical care medicine* 198, 497–508 (2018). [PubMed: 29533677]
3. Dickson RP, Erb-Downward JR, Martinez FJ & Huffnagle GB The Microbiome and the Respiratory Tract. *Annual review of physiology* 78, 481–504 (2016).
4. Marsland BJ & Gollwitzer ES Host-Microorganism Interactions in Lung Diseases. *Nat Rev Immunol* 14, 827–835 (2014). [PubMed: 25421702]
5. Wypych TP, Wickramasinghe LC & Marsland BJ The Influence of the Microbiome on Respiratory Health. *Nat Immunol* 20, 1279–1290 (2019). [PubMed: 31501577]
6. Lal CV et al. The Airway Microbiome at Birth. *Scientific reports* 6, 31023 (2016). [PubMed: 27488092]
7. Pammi M et al. Airway Microbiome and Development of Bronchopulmonary Dysplasia in Preterm Infants: A Systematic Review. *The Journal of pediatrics* 204, 126–133.e122 (2019). [PubMed: 30297287]

8. Segal LN et al. Randomised, Double-Blind, Placebo-Controlled Trial with Azithromycin Selects for Anti-Inflammatory Microbial Metabolites in the Emphysematous Lung. *Thorax* 72, 13–22 (2017). [PubMed: 27486204]
9. Ashley SL et al. Lung and Gut Microbiota Are Altered by Hyperoxia and Contribute to Oxygen-Induced Lung Injury in Mice. *Sci Transl Med* 12 (2020).
10. Jobe AJ The New Bpd: An Arrest of Lung Development. *Pediatric research* 46, 641–643 (1999). [PubMed: 10590017]
11. Walsh MC et al. Summary Proceedings from the Bronchopulmonary Dysplasia Group. *Pediatrics* 117, S52–56 (2006). [PubMed: 16777823]
12. Jensen EA & Schmidt B Epidemiology of Bronchopulmonary Dysplasia. *Birth Defects Res A Clin Mol Teratol* 100, 145–157 (2014). [PubMed: 24639412]
13. Madurga A, Mizíková I, Ruiz-Camp J & Morty RE Recent Advances in Late Lung Development and the Pathogenesis of Bronchopulmonary Dysplasia. *Am J Physiol Lung Cell Mol Physiol* 305, L893–905 (2013). [PubMed: 24213917]
14. Menon RT, Shrestha AK, Reynolds CL, Barrios R & Shivanna B Long-Term Pulmonary and Cardiovascular Morbidities of Neonatal Hyperoxia Exposure in Mice. *Int J Biochem Cell Biol* 94, 119–124 (2018). [PubMed: 29223466]
15. Park JR, Lee H, Kim SI & Yang SR The Tri-Peptide Ghk-Cu Complex Ameliorates Lipopolysaccharide-Induced Acute Lung Injury in Mice. *Oncotarget* 7, 58405–58417 (2016). [PubMed: 27517151]
16. Wang X et al. White Matter Damage after Chronic Subclinical Inflammation in Newborn Mice. *J Child Neurol* 24, 1171–1178 (2009). [PubMed: 19745089]
17. Shrestha AK et al. Consequences of Early Postnatal Lipopolysaccharide Exposure on Developing Lungs in Mice. *Am J Physiol Lung Cell Mol Physiol* 316, L229–L244 (2019). [PubMed: 30307313]
18. Yamada M, Fujino N & Ichinose M Inflammatory Responses in the Initiation of Lung Repair and Regeneration: Their Role in Stimulating Lung Resident Stem Cells. *Inflamm Regen* 36, 15 (2016). [PubMed: 29259688]
19. Iliodromiti Z et al. Acute Lung Injury in Preterm Fetuses and Neonates: Mechanisms and Molecular Pathways. *The journal of maternal-fetal & neonatal medicine : the official journal of the European Association of Perinatal Medicine, the Federation of Asia and Oceania Perinatal Societies, the International Society of Perinatal Obstet* 26, 1696–1704 (2013).
20. Moldoveanu B et al. Inflammatory Mechanisms in the Lung. *J Inflamm Res* 2, 1–11 (2009). [PubMed: 22096348]
21. Bender AT, Ostenson CL, Wang EH & Beavo JA Selective up-Regulation of Pde1b2 Upon Monocyte-to-Macrophage Differentiation. *Proc Natl Acad Sci U S A* 102, 497–502 (2005). [PubMed: 15625104]
22. Grommes J & Soehnlein O Contribution of Neutrophils to Acute Lung Injury. *Mol Med* 17, 293–307 (2011). [PubMed: 21046059]
23. Jobe AH & Ikegami M Mechanisms Initiating Lung Injury in the Preterm. *Early Hum Dev* 53, 81–94 (1998). [PubMed: 10193929]
24. Hütten MC, Wolfs TG & Kramer BW Can the Preterm Lung Recover from Perinatal Stress? *Mol Cell Pediatr* 3, 15 (2016). [PubMed: 27075524]
25. Balany J & Bhandari V Understanding the Impact of Infection, Inflammation, and Their Persistence in the Pathogenesis of Bronchopulmonary Dysplasia. *Frontiers in medicine* 2, 90 (2015). [PubMed: 26734611]
26. Willis KA et al. Perinatal Maternal Antibiotic Exposure Augments Lung Injury in Offspring in Experimental Bronchopulmonary Dysplasia. *Am J Physiol Lung Cell Mol Physiol* 318, L407–L418 (2020). [PubMed: 31644311]
27. Marsland BJ Regulating Inflammation with Microbial Metabolites. *Nature medicine* 22, 581–583 (2016).
28. Contrepois K, Liang L & Snyder M Can Metabolic Profiles Be Used as a Phenotypic Readout of the Genome to Enhance Precision Medicine? *Clin Chem* 62, 676–678 (2016). [PubMed: 26960666]

29. Sobie EA, Lee YS, Jenkins SL & Iyengar R Systems Biology--Biomedical Modeling. *Sci Signal* 4, tr2 (2011). [PubMed: 21917716]
30. Neu J Multiomics-Based Strategies for Taming Intestinal Inflammation in the Neonate. *Curr Opin Clin Nutr Metab Care* 22, 217–222 (2019). [PubMed: 30883466]
31. Bowler RP et al. New Strategies and Challenges in Lung Proteomics and Metabolomics. An Official American Thoracic Society Workshop Report. *Annals of the American Thoracic Society* 14, 1721–1743 (2017). [PubMed: 29192815]
32. Bos LD et al. Alterations in Exhaled Breath Metabolite-Mixtures in Two Rat Models of Lipopolysaccharide-Induced Lung Injury. *J Appl Physiol* (1985) 115, 1487–1495 (2013). [PubMed: 23908314]
33. Naz S, Garcia A, Rusak M & Barbas C Method Development and Validation for Rat Serum Fingerprinting with Ce-Ms: Application to Ventilator-Induced-Lung-Injury Study. *Anal Bioanal Chem* 405, 4849–4858 (2013). [PubMed: 23535741]
34. Shrestha AK et al. Interactive and Independent Effects of Early Lipopolysaccharide and Hyperoxia Exposure on Developing Murine Lungs. *Am J Physiol Lung Cell Mol Physiol* 319, L981–L996 (2020). [PubMed: 32901520]
35. Tesson BM, Breitling R & Jansen RC Diffcoex: A Simple and Sensitive Method to Find Differentially Coexpressed Gene Modules. *BMC Bioinformatics* 11, 497 (2010). [PubMed: 20925918]
36. Shrestha AK et al. Lung Omics Signatures in a Bronchopulmonary Dysplasia and Pulmonary Hypertension-Like Murine Model. *Am J Physiol Lung Cell Mol Physiol* 315, L734–L741 (2018). [PubMed: 30047283]
37. Chong J, Wishart DS & Xia J Using Metaboanalyst 4.0 for Comprehensive and Integrative Metabolomics Data Analysis. *Curr Protoc Bioinformatics* 68, e86 (2019). [PubMed: 31756036]
38. Pietrzyk JJ et al. Gene Expression Profiling in Preterm Infants: New Aspects of Bronchopulmonary Dysplasia Development. *PloS one* 8, e78585 (2013). [PubMed: 24194948]
39. Edgar RC Search and Clustering Orders of Magnitude Faster Than Blast. *Bioinformatics* 26, 2460–2461 (2010). [PubMed: 20709691]
40. Edgar RC Uparse: Highly Accurate Otu Sequences from Microbial Amplicon Reads. *Nat Methods* 10, 996–998 (2013). [PubMed: 23955772]
41. Quast C et al. The Silva Ribosomal Rna Gene Database Project: Improved Data Processing and Web-Based Tools. *Nucleic Acids Res* 41, D590–596 (2013). [PubMed: 23193283]
42. McMurdie PJ & Holmes S Phyloseq: An R Package for Reproducible Interactive Analysis and Graphics of Microbiome Census Data. *PloS one* 8, e61217 (2013). [PubMed: 23630581]
43. Anderson MJ A New Method for Non-Parametric Multivariate Analysis of Variance. *Austral Ecology* 26, 32–46 (2001).
44. Amara CS et al. Serum Metabolic Profiling Identified a Distinct Metabolic Signature in Bladder Cancer Smokers: A Key Metabolic Enzyme Associated with Patient Survival. *Cancer Epidemiol Biomarkers Prev* 28, 770–781 (2019). [PubMed: 30642841]
45. Vantaku V et al. Large-Scale Profiling of Serum Metabolites in African American and European American Patients with Bladder Cancer Reveals Metabolic Pathways Associated with Patient Survival. *Cancer* 125, 921–932 (2019). [PubMed: 30602056]
46. Gohlke JH et al. Methionine-Homocysteine Pathway in African-American Prostate Cancer. *JNCI Cancer Spectr* 3, pkz019 (2019). [PubMed: 31360899]
47. Jin F et al. Tobacco-Specific Carcinogens Induce Hypermethylation, DNA Adducts, and DNA Damage in Bladder Cancer. *Cancer Prev Res (Phila)* 10, 588–597 (2017). [PubMed: 28851690]
48. Whitlock M & D S in *The Analysis of Biological Data*, 2nd Ed (2015).
49. Package ‘Pheatmap’ 1.0.12. Dec 26, 2018. <https://Cran.R-Project.Org/Web/Packages/Pheatmap/Pheatmap.Pdf> (2018).
50. Grimm SL et al. Effect of Sex Chromosomes Versus Hormones in Neonatal Lung Injury. *JCI Insight* (2021).
51. Jobe AH & Bancalari E Bronchopulmonary Dysplasia. *American journal of respiratory and critical care medicine* 163, 1723–1729 (2001). [PubMed: 11401896]

52. Zoetis T & Hurtt ME Species Comparison of Lung Development. *Birth Defects Res B Dev Reprod Toxicol* 68, 121–124 (2003). [PubMed: 12866703]
53. Nagpal R et al. Comparative Microbiome Signatures and Short-Chain Fatty Acids in Mouse, Rat, Non-Human Primate, and Human Feces. *Front Microbiol* 9, 2897 (2018). [PubMed: 30555441]
54. Wagner BD et al. Airway Microbial Community Turnover Differs by Bpd Severity in Ventilated Preterm Infants. *PloS one* 12, e0170120 (2017). [PubMed: 28129336]
55. Lal CV et al. Early Airway Microbial Metagenomic and Metabolomic Signatures Are Associated with Development of Severe Bronchopulmonary Dysplasia. *Am J Physiol Lung Cell Mol Physiol* 315, L810–L815 (2018). [PubMed: 30113227]
56. Lohmann P et al. The Airway Microbiome of Intubated Premature Infants: Characteristics and Changes That Predict the Development of Bronchopulmonary Dysplasia. *Pediatric research* 76, 294–301 (2014). [PubMed: 24941215]
57. Gentle SJ et al. Bronchopulmonary Dysplasia Is Associated with Reduced Oral Nitrate Reductase Activity in Extremely Preterm Infants. *Redox Biol* 38, 101782 (2021). [PubMed: 33166868]
58. Fanos V et al. Urinary Metabolomics of Bronchopulmonary Dysplasia (Bpd): Preliminary Data at Birth Suggest It Is a Congenital Disease. *The journal of maternal-fetal & neonatal medicine : the official journal of the European Association of Perinatal Medicine, the Federation of Asia and Oceania Perinatal Societies, the International Society of Perinatal Obstet* 27 Suppl 2, 39–45 (2014).
59. Pintus MC et al. Urinary (1)H-Nmr Metabolomics in the First Week of Life Can Anticipate Bpd Diagnosis. *Oxid Med Cell Longev* 2018, 7620671 (2018). [PubMed: 30050661]
60. Piersigilli F & Bhandari V Metabolomics of Bronchopulmonary Dysplasia. *Clin Chim Acta* 500, 109–114 (2020). [PubMed: 31689411]
61. Huffnagle GB, Dickson RP & Lukacs NW The Respiratory Tract Microbiome and Lung Inflammation: A Two-Way Street. *Mucosal Immunol* 10, 299–306 (2017). [PubMed: 27966551]
62. Schmidt DR et al. Metabolomics in Cancer Research and Emerging Applications in Clinical Oncology. *CA Cancer J Clin* (2021).
63. Chang YC et al. Feedback Regulation of Aldoa Activates the Hif-1 α /Mmp9 Axis to Promote Lung Cancer Progression. *Cancer Lett* 403, 28–36 (2017). [PubMed: 28610954]
64. Tang Y, Yang X, Feng K, Hu C & Li S High Expression of Aldolase a Is Associated with Tumor Progression and Poor Prognosis in Hepatocellular Carcinoma. *J Gastrointest Oncol* 12, 174–183 (2021). [PubMed: 33708434]
65. Kang MK et al. Prognostic Significance of Genetic Variants in Glut1 in Stage Iii Non-Small Cell Lung Cancer Treated with Radiotherapy. *Thorac Cancer* 12, 874–879 (2021). [PubMed: 33522072]
66. Keeler AM et al. Airway Smooth Muscle Dysfunction in Pompe (Gaa $^{-/-}$) Mice. *Am J Physiol Lung Cell Mol Physiol* 312, L873–L881 (2017). [PubMed: 28336814]
67. Cross AS et al. Neu1 and Neu3 Sialidase Activity Expressed in Human Lung Microvascular Endothelia: Neu1 Restrains Endothelial Cell Migration, Whereas Neu3 Does Not. *J Biol Chem* 287, 15966–15980 (2012). [PubMed: 22403397]
68. Luzina IG et al. Elevated Expression of Neu1 Sialidase in Idiopathic Pulmonary Fibrosis Provokes Pulmonary Collagen Deposition, Lymphocytosis, and Fibrosis. *Am J Physiol Lung Cell Mol Physiol* 310, L940–954 (2016). [PubMed: 26993524]
69. Tada M, Takahashi S, Miyano M & Miyake Y Tissue-Specific Regulation of Renin-Binding Protein Gene Expression in Rats. *J Biochem* 112, 175–182 (1992). [PubMed: 1400260]
70. Khaliullin TO et al. Comparative Analysis of Lung and Blood Transcriptomes in Mice Exposed to Multi-Walled Carbon Nanotubes. *Toxicol Appl Pharmacol* 390, 114898 (2020). [PubMed: 31978390]

Impact Statement:

- Using multi-omics, identified and correlated key biomarkers of hyperoxia and LPS on murine lung micro-landscape; examined their potential clinical implication which show strong clinical relevance for future research.
- Using a double-hit model of clinical relevance to Bronchopulmonary Dysplasia, first to report integrated metabolomic/microbiome landscape changes and identify novel disease biomarker candidates.

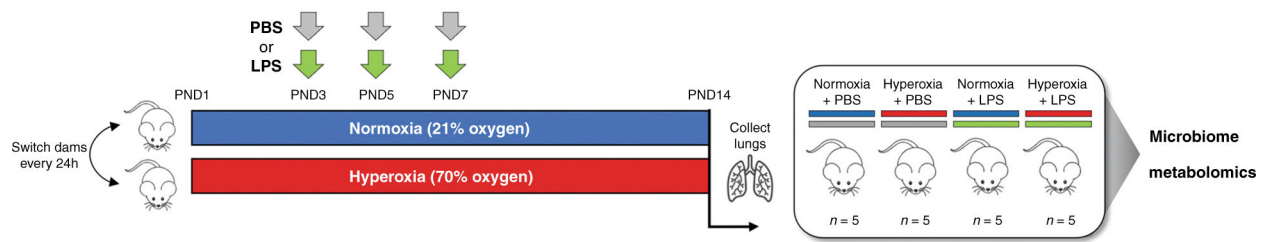


Figure 1. Analytical approach.

Wild-type C57BL/6J mice were exposed to a two-factor combination of room air/hyperoxia and PBS/LPS (n=5 per group). Lung microbiome was profiled using 16SrRNA sequencing and lung metabolome was profiled using targeted metabolomics via mass spectrometry. The effect of each individual exposure as well as of the hyperoxia/LPS interaction on the multi-modal omics profiles were analyzed via 2-way ANOVA. Differential co-expression analysis (DiffCoEx) revealed both single-omic and multi-omics modules affected significantly by the individual exposures.

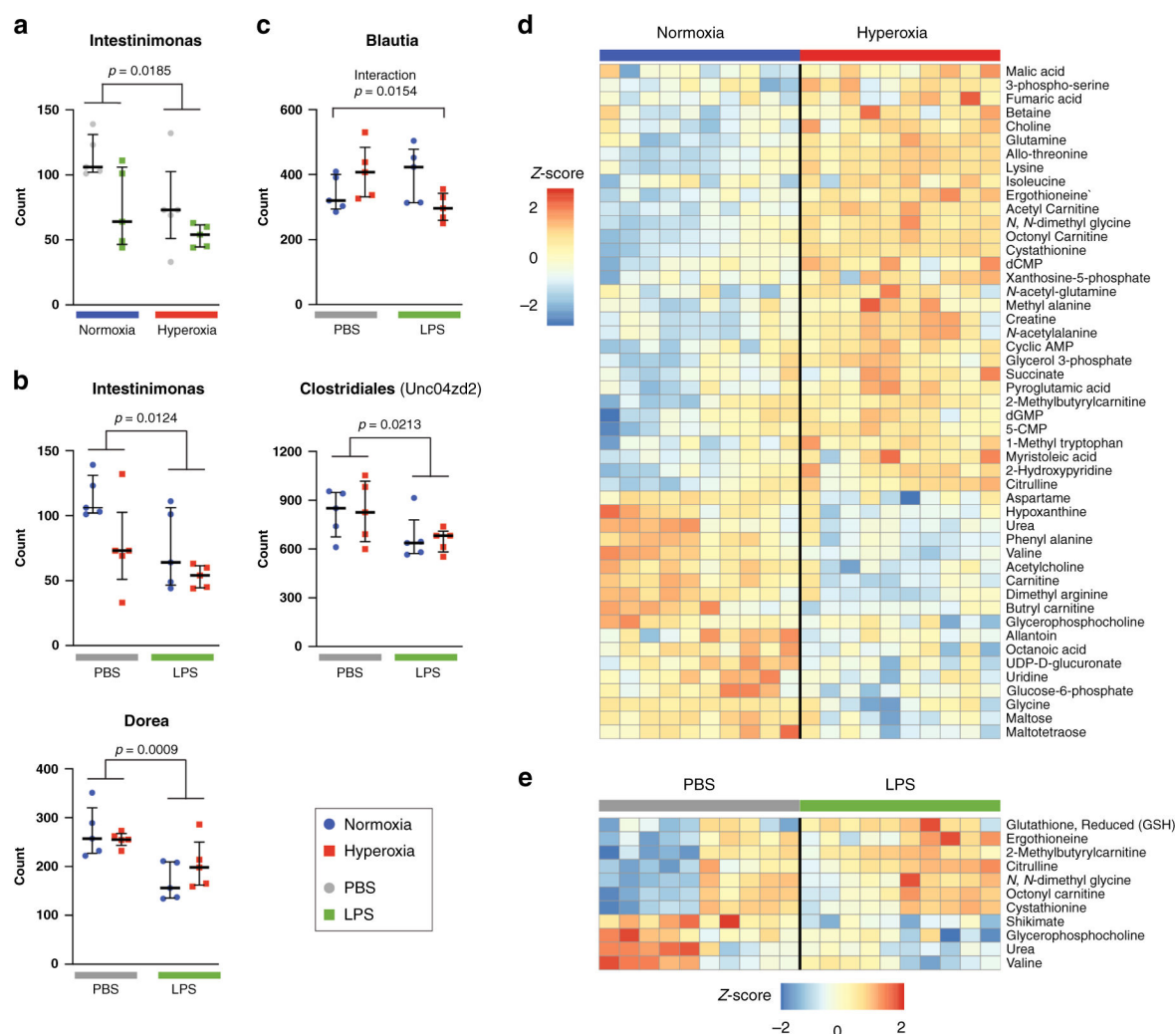


Figure 2. Hyperoxia and LPS exposures alter the microbial and metabolomic landscapes. 2-way ANOVA was used to determine microbiome genera associated with (A) hyperoxia exposure (B) LPS exposure and (C) interaction between exposures. Only genera above 0.5% abundance of the overall microbial community were used. 2-way ANOVA was used to determine metabolites associated with (D) hyperoxia exposure (E) LPS exposure.

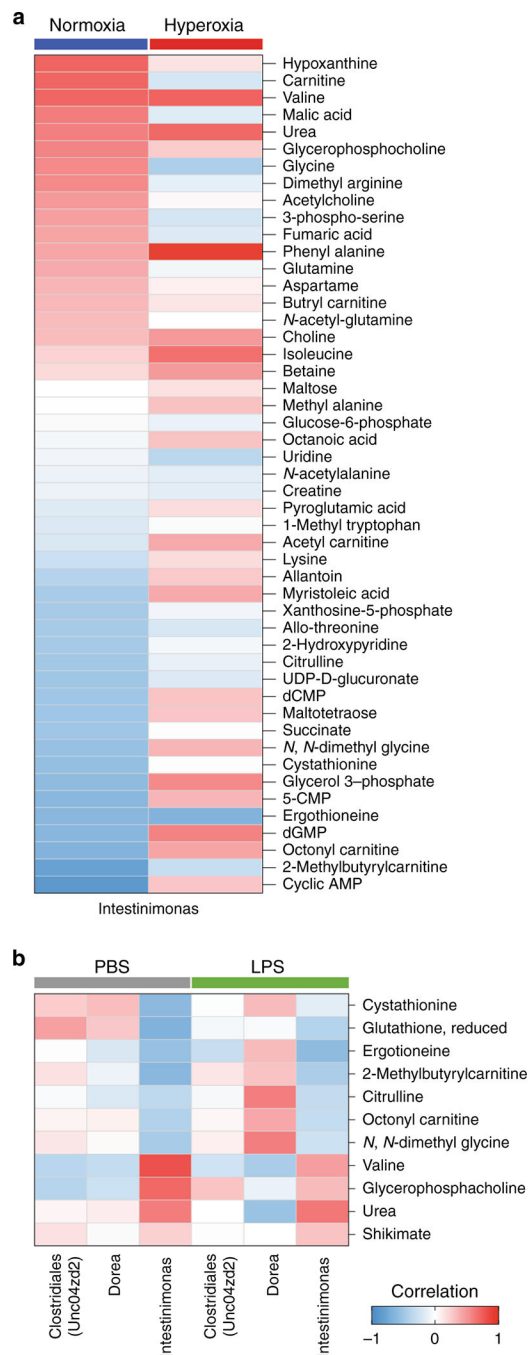


Figure 3. Microbiome-metabolite correlation for individual exposure-associated microbiome genera and metabolites.

(A) Spearman rank correlations were computed for microbiome genera and metabolites associated with hyperoxia exposure in each of the normoxia and hyperoxia sample groups. (B) Spearman rank correlations were computed for microbiome genera and metabolites associated with LPS exposure in each of the PBS and LPS sample groups

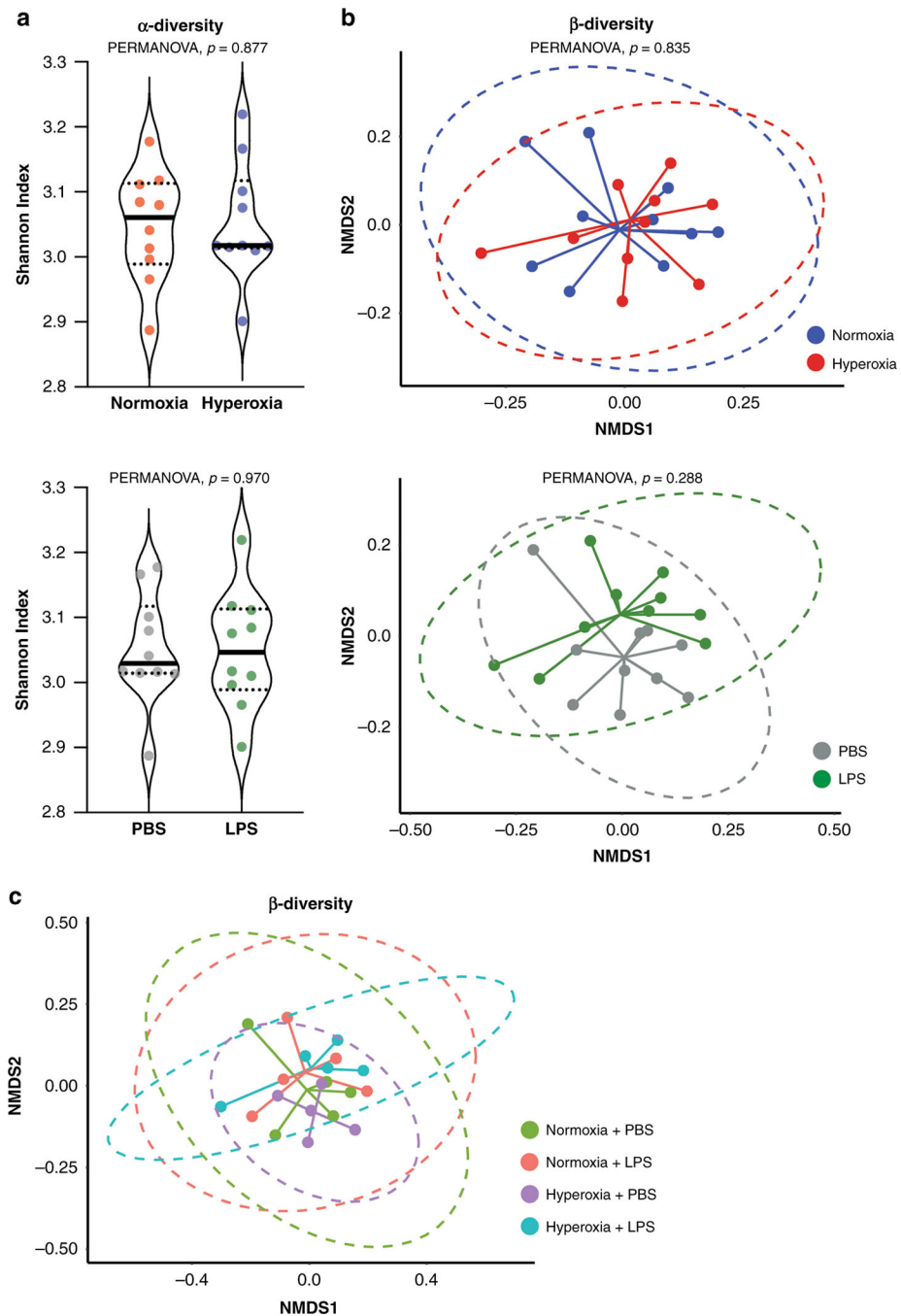


Figure 4. The impact of individual hyperoxia and LPS exposures on microbiome diversity in murine lung.

(A) Impact of hyperoxia and LPS exposures on α -diversity (Shannon index). (B) Impact of hyperoxia and LPS exposures on β -diversity (Bray-Curtis index visualized with non-metric multidimensional scaling (NMDS)). (C) Global impact of 4 experimental groups of the 2-hit mouse model on β -diversity.

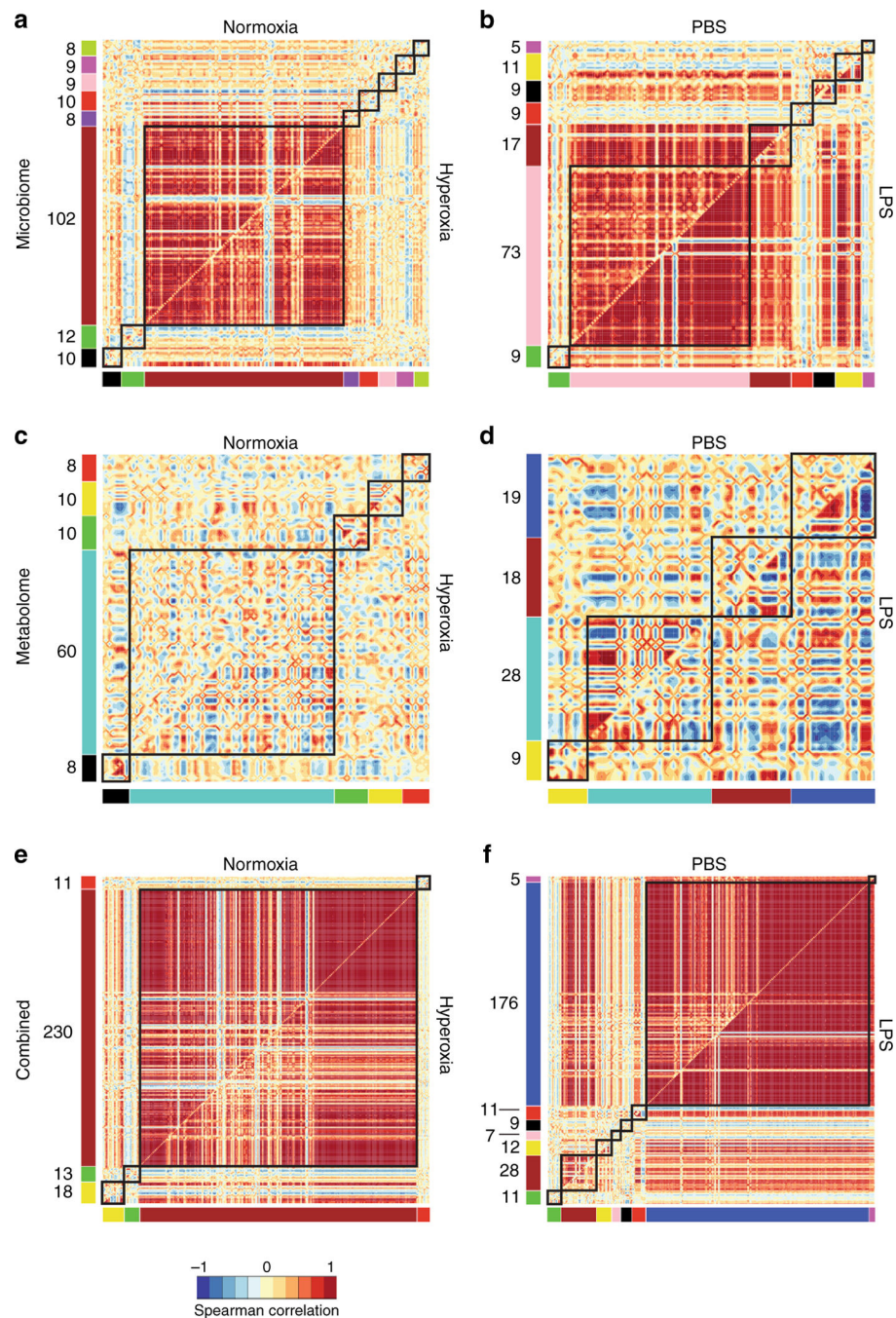


Figure 5. Differential correlation for single-omic and multi-omic microbiome and metabolomic modules induced by either hyperoxia or LPS exposures.

Differentially correlated modules between normoxia and hyperoxia exposures for (A) microbiome genera (C) metabolites (E) multi-omics microbiome genera and metabolomics profiles. Differentially correlated modules between PBS and LPS exposures for (B) microbiome genera (D) metabolites (F) multi-omics microbiome genera and metabolomics profiles. Heatmaps depict Spearman rank correlations between features (microbiome genera, metabolites, or multi-omic profiles). Number of features in each modules were indicated. Modules were highlighted via square overlays for the convenience of the reader.

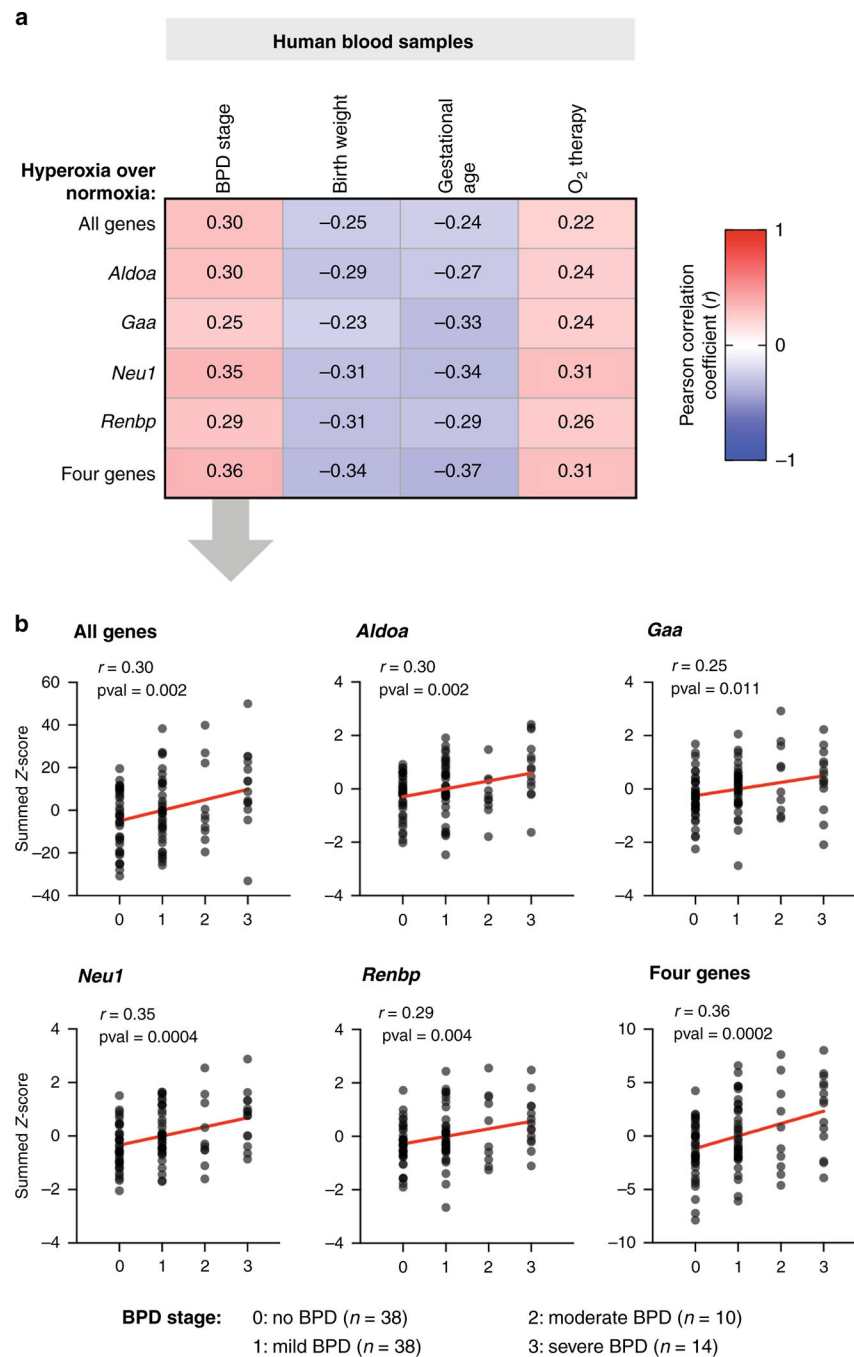


Figure 6. A murine integrated transcriptomics/metabolomic signature of hyperoxia associates with blood transcriptome in human newborns at high-risk for BPD.

A. Blood transcriptome from human newborns at risk for BPD was collected at PND28. We identified several clinical variables of interest, including BPD status, birth weight, gestational age, and the requirement for oxygen. A publicly available age-matched murine hyperoxia signature showed association with all four clinical variables. We identified four genes associated with metabolites altered in our murine model. *Aldoa*, *Gaa*, *Neu1*, and *Renbp* associate individually and as a gene signature positively with BPD status and need for oxygen and negatively with birth weight and gestational age. The heatmap shows

Pearson Correlation Coefficients, with significance achieved at $p < 0.05$. B. Scatterplots showing the distribution of signatures scores in newborns at PND28 grouped by BPD status.

Author Manuscript

Author Manuscript

Author Manuscript

Author Manuscript

Table 1.

Summary of microbiome genera and metabolites significantly associated with hyperoxia exposure, LPS exposure, or the interaction of the two exposures.

	Number of significant genera		Number of significant metabolites	
Comparison	Increased abundance	Decreased abundance	Up regulated	Down regulated
Hyperoxia vs Normoxia	1	0	31	18
LPS vs. PBS	0	3	7	4
Interaction	1		8	

p-value<0.05 and abundance>0.5% was used for microbiome analysis. FDR<0.05 was used for metabolomics analysis.